An Extended Pattern Search Approach to Wind Farm Layout Optimization

Bryony L. Du Pont
e-mail: bryony@cmu.edu

Jonathan Cagan
e-mail: cagan@cmu.edu

Integrated Design Innovation Group,
Department of Mechanical Engineering,
Carnegie Mellon University,
Pittsburgh, PA 15213

An extended pattern search approach is presented for the optimization of the placement of wind turbines on a wind farm. Problem-specific extensions infuse stochastic characteristics into the deterministic pattern search, inhibiting convergence on local optima and yielding better results than pattern search alone. The optimal layout for a wind farm is considered here to be one that maximizes the power generation of the farm while minimizing the farm cost. To estimate the power output, an established wake model is used to account for the aerodynamic effects of turbine blades on downstream wind speed, as the oncoming wind speed for any turbine is proportional to the amount of power the turbine can produce. As turbines on a wind farm are in close proximity, the interaction of turbulent wakes developed by the turbines can have a significant effect on the power development capability of the farm. The farm cost is estimated using an accepted simplified model that is a function of the number of turbines. The algorithm develops a two-dimensional layout for a given number of turbines, performing local turbine movement while applying global evaluation. Three test cases are presented: (a) constant, unidirectional wind, (b) constant, multidirectional wind, and (c) varying, multidirectional wind. The purpose of this work is to explore the ability of an extended pattern search (EPS) algorithm to solve the wind farm layout problem, as EPS has been shown to be particularly effective in solving multimodal layout problems. It is also intended to show that the inclusion of extensions into the algorithm can better inform the search than algorithms that have been previously presented in the literature. Resulting layouts created by this extended pattern search algorithm develop more power than previously explored algorithms using the same evaluation models and objective functions. In addition, the algorithm's resulting layouts motivate a heuristic that aids in the manual development of the best layout found to date. The results of this work validate the application of an extended pattern search algorithm to the wind farm layout problem, and that its performance is enhanced by the use of problem-specific extensions that aid in developing results that are superior to those developed by previous algorithms. [DOI: 10.1115/1.4006997]

Introduction

According to the U.S. Department of Energy (DOE), "Increased R&D efforts and innovation will be required to continue to expand the wind energy industry" in the United States, where wind power is still a maturing technology [1]. The optimization of wind farm layouts is part of this R&D effort. The DOE estimates that the demand for energy will increase by 39% in the next twenty years [1] with the intent of supplying 20% of the total electricity demand utilizing wind power. In addition, outdated means of energy development have been attributed to climate change, pollution, and permanent depletion of natural resources. These concerns have led to public demand for cleaner, sustainable energy sources like wind turbine technology. To meet these demands it will be necessary to ensure new wind farm installations are developing as much power as possible, which depends on the wind farm layout's capability to account for local wind conditions and aerodynamic interaction between turbines.

The complexity of the wind farm layout problem lies in the dynamic conditions of the farm site and the modeling available to represent realistic wind patterns and wake interactions. A turbine in wind will develop a turbulent wake that decreases the wind speed downstream. On a wind farm, turbines are typically placed in close enough proximity that the effect of placement in a wake could drastically reduce the effective wind speed to downstream turbines and therefore decrease their power output. Essentially, the goal is to incorporate as many turbines as possible while minimizing land use, without compromising the efficiency of the farm due to wind speed decrement from wake interactions. This work seeks to develop an optimization algorithm that will consider these complexities and improve upon previously explored methods to provide optimal wind farm layouts.

Previous Approaches

The first attempt at applying computational optimization algorithms to the wind farm layout problem was by Mosetti et al. [2], utilizing a genetic algorithm (GA). This preliminary study developed the framework that has been continuously used for comparison purposes, including the objective function formula and the use of the Jensen wake model [3]. Mosetti et al. used a discretized solution space of 100×100 cells and limited the placement of turbines to the center of each cell. The genetic algorithm considers each row of the grid as a binary string. A similar but improved GA approach was performed by Grady et al. [4] whose algorithm incorporated heuristic knowledge about wind farms and utilized more advanced computational resources. Two more recent studies, one by Wan et al. [5] and one by Mittal [6] improved on both previous genetic algorithm approaches by implementing a second discretization phase that allowed the turbines to be moved within their assigned cells. Though these works have advanced the study of wind farm layout optimization, these genetic algorithms may have been hindered by the inherent discretization of their binary

Contributed by the Design Automation Committee of ASME for publication in the JOURNAL OF MECHANICAL DESIGN. Manuscript received March 14, 2011; final manuscript received May 2, 2012; published online July 23, 2012. Assoc. Editor: Wei Chen.

chromosomes, which directly affects the final precision of the objects in a layout problem. In order to fairly compare the performance of these GA approaches with the current EPS, an additional analysis has been developed using the EPS that is constrained to perform in the same discretized solution space as given by Refs. [2] and [4].

Approaches aside from genetic algorithms have also been applied to the wind farm layout problem. Marmidis et al. [7] employed a Monte Carlo method, which relies on the use of random turbine placement. In this study, turbines were randomly placed on the same 100×100 grid used in previous GA approaches and then evaluated, with this process iterating until certain stopping criteria were met. Though Marmidis et al. reported better results than prior approaches, considerable differences in evaluation and visual analysis of their resulting layouts imply discrepancies in reported results. Bilbao and Alba [8] developed a simulated annealing (SA) algorithm that produced better layout evaluations when directly compared to a distributed genetic algorithm (DGA) approach concluded by Huang [9]. Though Bilbao and Alba's simulated annealing algorithm and Huang's distributed genetic algorithm have the objective of maximizing farm profit, their disclosure of power, efficiency, and layout coordinates allows for comparison to the current work. However, both of these algorithms exhibit similar precision deficiency as the previous genetic algorithm approaches due to the use of a discretized solution space.

Additional approaches to solving the wind farm layout problem have been developed that are not used in the current work because they preclude a direct comparision of resulting layouts from the EPS algorithm to other wind farm layout literature. Elkinton et al. [10] established the framework for offshore wind farm layout, the OWFLO (Offshore Wind Farm Layout Optimization) project in 2006. In offshore wind farm development, costs are different than those of onshore farms, so modeling the operations and maintenance costs, availability costs, support structure costs, and electrical interconnection costs are paramount. Therefore, the OWFLO work uses the Opti-OWECS (the Structural and Economic Optimization of Bottom-Mounted Offshore Wind Energy Converters) and OWECOP (Offshore Wind Energy—Cost and Potential) models to determine the cost of energy, unlike the cost modeling used in the current work. Other works that relate solely to offshore wind farms are not referenced herein as the complexities of offshore modeling and costs create difficulty in direct comparison.

Multiple advances using evolutionary algorithm approaches (such as genetic algorithms) to the wind farm layout problem have been conducted. Sisbot et al. [11] used a multi-objective genetic algorithm and a cost model that was specifically geared for the type of turbine being proposed, as well as the PARK wake model used in the current work, but used the prevailing wind directions and speed from the actual wind farm site, Another genetic algorithm approach performed by Emami and Noghreh [12] used the same wake modeling and cost modeling as the current work, but used cost as a constraint, and were able to develop layouts that were specifically optimized for various cost totals. Work by Kusiak and Zheng [13] optimized both total power and power factor (but not cost), and found the optimal resulting settings for blade pitch angle and rotor torque using an evolutionary algorithm in conjunction with data mining. Gonzalez et al. [14] also used an evolutionary algorithm, but optimized cost by incorporating initial capital investment and operation and maintenance costs, and can incorporate exclusion zones and available investment as constraints. Saavedra-Moreno et al. [15] showed that seeding an evolutionary algorithm with a heuristic approach led to improvements in performance over evolutionary algorithms alone when applied to the wind farm layout optimization problem.

Work involving particle swarm optimization was performed by Chowdhury et al., [16] using a variable axial induction factor and the ability to vary turbine rotor diameters and was directly compared with wind tunnel data for a model farm. Additionally, a combinatorial optimization approach was undertaken by Muskaterov and Borissova [17], which utilized commercial wind turbine geometries and used both investment cost and total power as objectives. An biology-inspired approach mimicking the replication of viruses was applied by Ituarte-Villarreal and Espiritu [18], showing promise compared with Mosetti et al.'s genetic algorithm approach.

It is pertinent to explore applying an EPS algorithm to the wind farm layout problem, in that EPS is specifically designed to explore problems with multimodal solution spaces [19]. The extended pattern search combines the effectiveness of deterministic algorithms with the global exploration capability of stochastic methods, which can lead to increases in efficiency and thus the energy output of the farm. The wind farm layout optimization problem is similar to a 2D product packaging problem, where objects (turbines) must be placed without interference, according to a performance objective, within an established solution space. The successful application of EPS to the 2D and 3D layout of products and packages [19,20] suggests the potential for success in application to the wind farm layout optimization problem. In addition, Yin and Cagan [19] showed that an extended pattern search algorithm was more computationally efficient than a comparable genetic algorithm, further suggesting the potential success of the application of EPS to the wind farm layout problem. In sum, we view the wind farm layout problem as an isomorph of the 2D product layout problem. The use of EPS is further justified by the algorithm's use of a continuous solution space, allowing for precise movement throughout the course of the search. The EPS algorithm can develop multiple equally-evaluating layouts, and given the potential establishment of the layout in a dynamic, real-world environment, the ability to select from multiple high performing layouts may be ideal.

The goal of this work is to extend and apply the extended pattern search on a wind farm layout and determine how the results compare to previous attempts to solve this problem. The following section of this paper will describe the details of the wake modeling (which determines power) and cost modeling. Next, the methodology of the extended pattern search is discussed, followed by a description of the numerical procedure of this particular problem. Lastly, results of this study are presented and compared to previous work and conclusions about the algorithm's performance are drawn.

Wake and Cost Modeling

A wake model is a simplified quantitative means of representing the fluid interaction between turbines. The wake developed by a turbine in wind greatly reduces the wind speed immediately behind the rotor, increasing slowly with distance downstream, as shown in Fig. 1. The wake model accounts for wake interactions and develops the effective wind speed—the oncoming wind speed

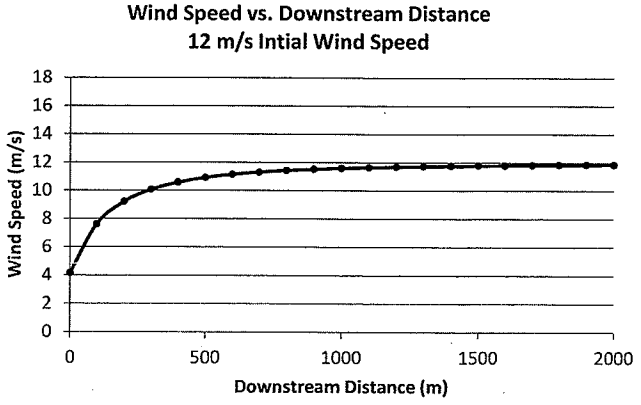

Fig. 1 Immediate speed reduction and eventual asymptotic approach to initial windspeed (12 m/s) within a wake

at any turbine after wake speed deficits from upstream turbines have been incorporated. The current EPS algorithm utilizes the wake model developed by Jensen [3], in an effort to facilitate comparison to previous wind farm layout work that also uses this model. For this same reason, it should be noted that this model is used as originally written, and the current work does not seek to improve or alter the wake model.

This effective wind speed determines the power output of the rotor—generally, the higher the wind speed, the more power a turbine can produce. With the assumption that momentum is conserved inside the wake, a momentum balance is established:

$$\pi r_r^2 v + \pi\left(r_1^2 - r_r^2\right)u_0 = \pi r_1^2 u \tag{1}$$

where r_r is the rotor radius, u_0 is the ambient wind speed, v is the wind speed just behind the rotor, r_1 is the effective downstream radius of the wake, and u is the wind speed in the wake downstream of a turbine at distance x, as seen in Fig. 2.

Assuming a linear relationship between x and r_1 (as indicated by the triangular wake) and employing the theory that assumes the wind speed directly behind the rotor is $\simeq 1/3$ of the oncoming wind speed [3], Eq. (1) can be solved for the downstream wind speed u:

$$u = u_0\left(1 - \frac{2}{3}\left(\frac{r_r}{r_1}\right)^2\right) \tag{2}$$

where r_1 is related to the turbine rotor radius r_r by a linear relationship with downstream distance x:

$$r_1 = r_r + \alpha x \tag{3}$$

where α is known as the entrainment constant and is given by

$$\alpha = \frac{0.5}{\ln(z/z_0)} \tag{4}$$

where z is the hub height of the turbine and z_0 is the surface roughness of the ground. Formula (3) is used to discern whether a turbine is in the wake of an upstream turbine. Alternatively, a variant but nearly identical formulation for effective wind speed has also been used [2,5]

$$u = u_0\left(1 - \frac{2a}{\left(1 + \alpha\left(\frac{x}{r_1}\right)\right)^2}\right) \text{ where } r_1 = r_r\sqrt{\frac{1-a}{1-2a}} \tag{5}$$

where a is the axial induction factor.

For the case of turbines located in multiple wakes, the effective wind speed is calculated by summing the kinetic energy deficits of the individual wakes. The effective wind speed for a turbine in n wakes is calculated using the following expression:

$$u = u_0\left[1 - \sqrt{\sum_{i=1}^{n}\left(1 - \frac{u_i}{u_0}\right)^2}\right] \tag{6}$$

These formulae indicate three distinct means of developing the effective wind speed for each turbine: (1) If the turbine has no upstream turbines, the effective wind speed is the ambient wind speed; (2) If the turbine is located in one wake, formulas (2) or (5) are used; and (3) if the turbine has multiple upstream turbines and is therefore located in multiple wakes, formula (6) is used. The effective wind speeds of each turbine are utilized to develop a total power estimate for the N turbines on the farm, given by

$$P_{\text{tot}} = \sum_{i=1}^{N} 0.3u_i^3 \tag{7}$$

The power formula stated in Eq. (7) is duplicated directly from Mosetti et al. [2], for comparison purposes. More accurate power modeling formulae exist in the literature [21], and the coefficient of 0.3 is likely an estimation of the incorporation of turbine geometry, air density, and power coefficient.

It is also necessary to minimize the cost of turbine installation and use. Mosetti et al. [2] established an expression for estimating the cost of a farm per year, based solely on the number of turbines N:

$$\text{cost} = N\left(\frac{2}{3} + \frac{1}{3}e^{-0.00174N^2}\right) \tag{8}$$

This expression is normalized, where each turbine has a cost of 1. This expression incorporates a cost reduction for the installation of larger-N farms; other factors that may be included are not specifically noted by Mosetti et al.

The objective function for the wind farm layout optimization must maximize the power output of the farm while minimizing cost. Therefore, the objective function is given by

$$\text{Objective} = \frac{\text{cost}}{P_{\text{tot}}} \tag{9}$$

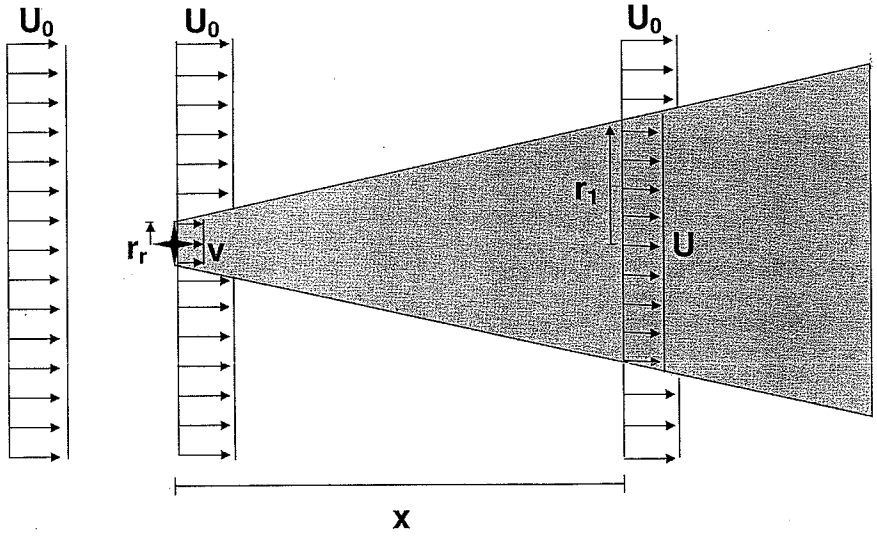

Fig. 2 Schematic of wake model

The optimization algorithm will search for the minimum value of this objective function.

It should be noted that the use of this model suggests inherent simplification of the results, as the model itself uses an idealized semblance of the wake profile and behavior [22]. In particular, the wind speeds within a wake are considered constant across the width of the wake for a given downstream distance, whereas the lines of constant wind speed taking on the shape of a Gaussian distribution would be more accurate. Similarly, there is an "on/off" characteristic about the wake boundary that belies the more realistic wind speed gradient at the edges. Additionally, this model cannot account for the complex turbulent flow directly behind and caused by the rotor blades, and as such the wake effects of the near-wake region are unrealistic. However, given the minimum proximity constraint between turbines, this shortcoming most likely does not significantly affect the optimization. The cost modeling formulation is also considerably simplified, and future work will incorporate more accurate modeling that accounts for more parameters (i.e., cost changes based on turbine design, interconnectivity costs, farm site costs, etc.).

Extended Pattern Search Methodology

The wind farm layout problem has characteristics that require nondeterministic strategies to effectively solve. The space is multimodal as was verified by running a deterministic search algorithm with randomized initial layouts that produced inferior results to our EPS approach. Although various stochastic methods such as genetic algorithms (as used by Mosetti et al. [2] and Grady et al. [4]), distributed genetic algorithms [9], simulated annealing [8] and others are feasible, the benefits of the EPS algorithm are described as follows.

Pattern search algorithms are deterministic search methods that use a set pattern of search directions in order to find an optimal placement [23]. Pattern search is a direct search method in that it traverses a sequence of trial solutions, maintaining the best evaluation and comparing it directly to each subsequent evaluation, without the need to evaluate derivatives. At every potential move in the pattern, the objective function is evaluated and compared to the best prior evaluation, only selecting moves that result in an improved objective value. Constraints that prohibit the infeasible placement of turbines are enforced with every move. Each move spans a set step size, which is initially defined with respect to the size of the solution space to allow for broad movement. Once every turbine has remained stationary through all pattern directions (in this case, along the coordinate axes) at a given step size, the step size is halved and the search is repeated. The search exits when no possible moves for any turbine have developed an improvement in the objective function evaluation at a minimum allowable step size.

In order to avoid converging on local minima (a common pitfall of deterministic algorithms), extensions are employed that add stochasticity to the system [19]. That is, though the search is fundamentally based in the rigid generalized pattern search, subalgorithms that employ randomized characteristics selectively "liberate" the search at certain points throughout the algorithm to expand the search space and potentially escape local optima. Similar to the results of the extended pattern search of Yin and Cagan for 3D layout optimization [19], the addition of extensions to the pattern search have yielded improvement in results compared to a generalized pattern search (without extensions) applied to the same problem. These extensions improve wind farm efficiency, the likelihood of developing a 100% efficient layout, and increase the total power development of the farm, Understanding of the algorithm is best facilitated by a detailed description of the extended pattern search, including extensions, expressed as the flowchart in Fig. 3 for this application.

Following the method of Yin and Cagan [19], the extensions to the pattern search are indicated in the flow chart by capital letters. The first extension is the use of a random initial layout. The only restriction on the initial layout is the same constraints applied to every trial move—a turbine cannot be placed within five rotor diameters of another turbine or outside of the solution space. The second extension is the randomized selection order of turbines. This ensures that no turbine's individual movement is favored over another. The final extension is the popping algorithm that performs once all turbines have stopped moving at the current step size. A number of the weakest performing turbines (based on the local objective of individual power output) are "popped" to a random location. The new locations are kept if they do not cause interference and improve the evaluation. The popping algorithm exits after a given number of pop attempts are made or an improved location is found for each of the selected weak turbines. For the wind farm layout problem, the popping algorithm parameters were determined empirically, with 5 weak-performing turbines potentially being moved to new random locations, utilizing up to 1000 random new location attempts. The design of the popping algorithm is such that re-evaluation is performed at each potential move; therefore if a weak-performing turbine is not relocated within its given number of movement attempts or is not moved to a substantially superior location, that same turbine will again re-evaluate as weak, and will be run through the extension again.

Problem Formulation

The extended pattern search algorithm uses a continuous solution space, the benefit of which is made evident by the minimum distance requirement between turbines to avoid interference. In the discretized solution spaces of previous works [2,4,6–9], the five rotor diameter minimum distance is inherently satisfied in the directions along the X and Y axes by locating turbines in the center of each cell. However, turbines in diagonally adjacent cells are actually further apart than the specified minimum distance, as shown in Fig. 4(*a*). The continuous solution space allows for turbines to be placed at the true minimum distance in any direction, as shown in Fig. 4(*b*). As it is the purpose of this work to establish the performance of the EPS algorithm with respect to previous algorithms that utilize a discretized solution space, a brief comparison of the EPS constrained to perform within the same discretized solution space as these algorithms is stated in the results.

In the example included in this paper, the solution space is 2 km by 2 km, and the turbine geometry consists of a 60 m hub height and a 40 m rotor diameter. The surface roughness is taken to be 0.5 m and is constant. Case (a) is that of constant wind speed (12 m/s) and unidirectional wind (from the bottom of the field in the +Y direction), as shown in Fig. 5(*a*). Case (b) also has constant 12 m/s wind speed, but the wind is considered from 36 rotational directions (in 10 deg increments) with equivalent probabilities of occurrence, as shown in Fig. 5(*b*). Case (c), the most complex and realistic wind case, considers three wind speeds (8, 12, and 17 m/s) and the same 36 rotational directions, and both wind speed and direction are of varying probabilities of occurrence, as shown in Fig. 5(*c*).

Considering there are no restrictions on turbine placement (apart from avoiding interference), it is necessary to systematically determine which turbines are located in the wakes of upstream turbines. For each turbine the maximum width of its wake (based on its distance from the back of the field) is found and a rectangular neighborhood of that width is created. The turbines that lie in this wake are then flagged, and the upstream distance between each of them and the wake-producing turbine is calculated. Using Eq. (3), the actual width of the triangular wake r_1 is determined for each flagged turbine, and only those within this width at their current downstream distance are further considered to be affected by that wake. The initial step size chosen is 400 m and is halved until reaching a minimum value of 3.125 m. It was determined for this particular study

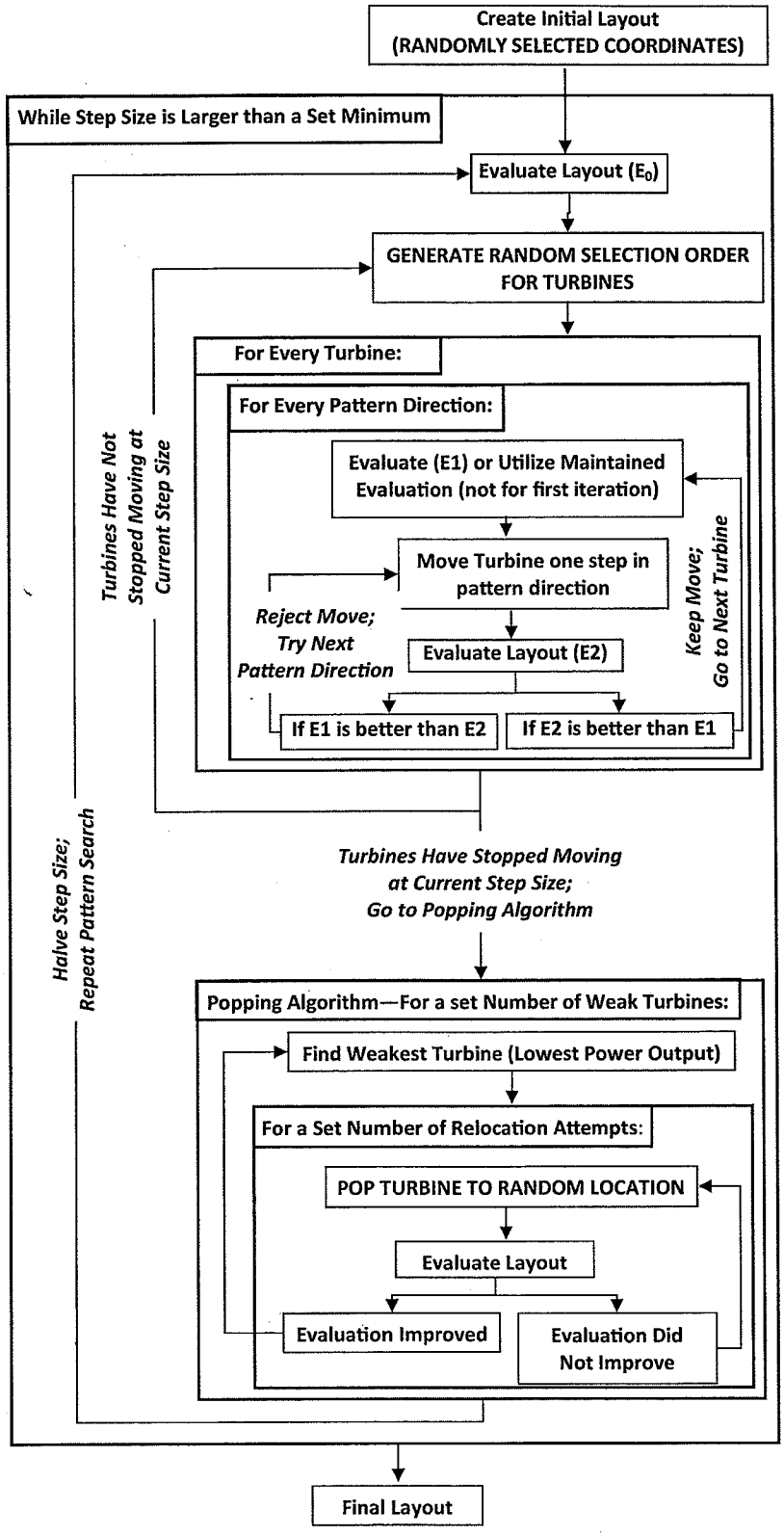

Fig. 3 Flowchart for current EPS

that an initial step size of 1/5 of the length of the solution space allowed for enough broad movement to thoroughly explore the space, while reduction by half at each iteration yielded precise local movement. The popping algorithm attempts to relocate the worst performing turbine five times, using up to 1000 random locations depending on the number of turbines in the layout.

The optimization problem is formalized as:

$$\text{Minimize } \frac{\text{cost}}{\text{Power}_{\text{Total}}} = \frac{N\left(\frac{2}{3}+\frac{1}{3}e^{-0.00174N^2}\right)}{\sum_{i=1}^{N} 0.3u_i^3}$$

$$\text{where } u_i = \begin{cases} U_A = u_0 & U_A : \text{turbine in no wakes} \\ U_B = u_0\left(1 - \frac{2}{3}\left(\frac{r_r}{r_r + \left(\frac{0.5}{\ln(z/z_0)}\right)x}\right)^2\right), & \text{where} \quad U_B : \text{turbine in one wake} \\ U_C = u_0\left[1 - \sqrt{\sum_{i=1}^{n}\left(1 - \frac{U_B}{u_0}\right)^2}\right] & U_C : \text{turbine in multiple wakes} \end{cases}$$

With respect to X Location x, Y Location y, and number of turbines N,

Such that: No turbines are placed outside of the solution space boundary.

No turbine is positioned within 200 m (5D) of another turbine.

$$0 \le x \le 2000m,$$

$$0 \le y \le 2000m,$$

$$26 \le N \le 80 \quad \text{for case (a), and}$$
$$15 \le N \le 60 \quad \text{for cases (b) and (c)}$$

Results and Discussion

Quantitative comparison between the extended pattern search results and the results of previous approaches was developed, including an efficiency percentage (percent at which the farm's power development represents the maximum amount of power possible given the wind conditions and geometry of the turbine). For a given turbine hub height and rotor diameter, and for a given wind speed, a 100% efficient turbine will have an effective wind speed equal to the ambient oncoming wind speed (the turbine is not located in a wake). A 100% efficient layout consists entirely of 100% efficient turbines. It is important to note that it is not realistically possible for a wind farm to be 100% efficient, and given the simplifications of the current modeling, what is reported as a 100% efficient layout is only theoretically so, and only relevant to the current problem formulation. It should be noted that the problem formulation of previous literature was purposely retained in the current work to enable direct comparison, specifically limited to those to which total power development, efficiency, and actual layout coordinates can be contrasted [2,3,8,9]. Additionally, each of the previous results to which the current work is compared use identical, unaltered turbine geometry. Comparisons to previous results are shown, first by indicating an EPS layout of the same number of turbines as those from previous work, followed by the optimal EPS layout for each case. As the EPS has stochastic characteristics, it is not guaranteed to converge on the same solution over multiple runs. Following common practice with such algorithms, the EPS was performed ten times at every number of turbines for a set range (26–80 turbines for case (a), and 15–60 turbines for cases (b) and (c)), and the best solution, along with the standard deviation across the ten solutions, is reported.

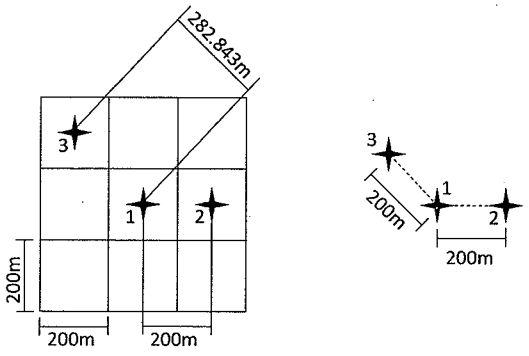

(a) Representation from previous work (b) Current representation

Fig. 4 Comparison of solution spaces—(*a*) discretized and (*b*) continuous

EPS for Discretized Solution Space. Prior to discussion of the results of this work, it is important to disclose the performance of the EPS using a discretized solution space. As previously stated, some of the algorithms to which the EPS is being compared perform within a discretized solution space: a 10×10 grid that limits the potential placement of a turbine to the center of a grid cell (resulting in only 100 possible locations). Though the EPS is designed to use a continuous solution space as a benefit to the search (as depicted in Fig. 4), constraining it to use the discretized solution space indicates how the EPS compared with these previous algorithms. Comparison to the case (a) results of Mosetti et al. is

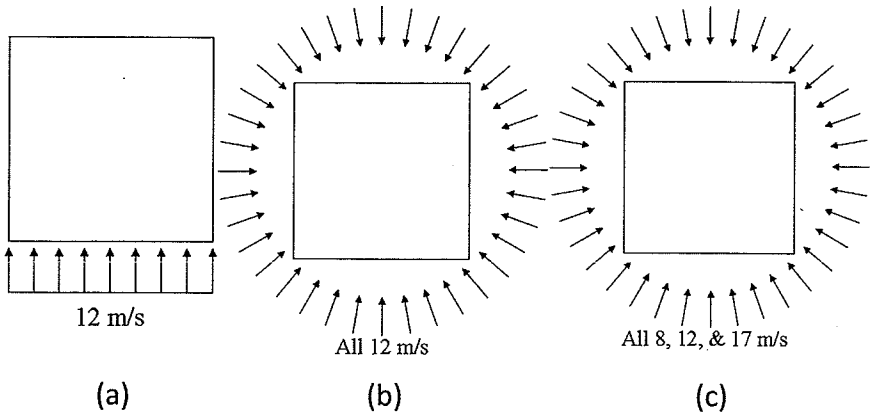

Fig. 5 Illustration of wind directions and speed—(*a*) case a, (*b*) case b, and (*c*) case c

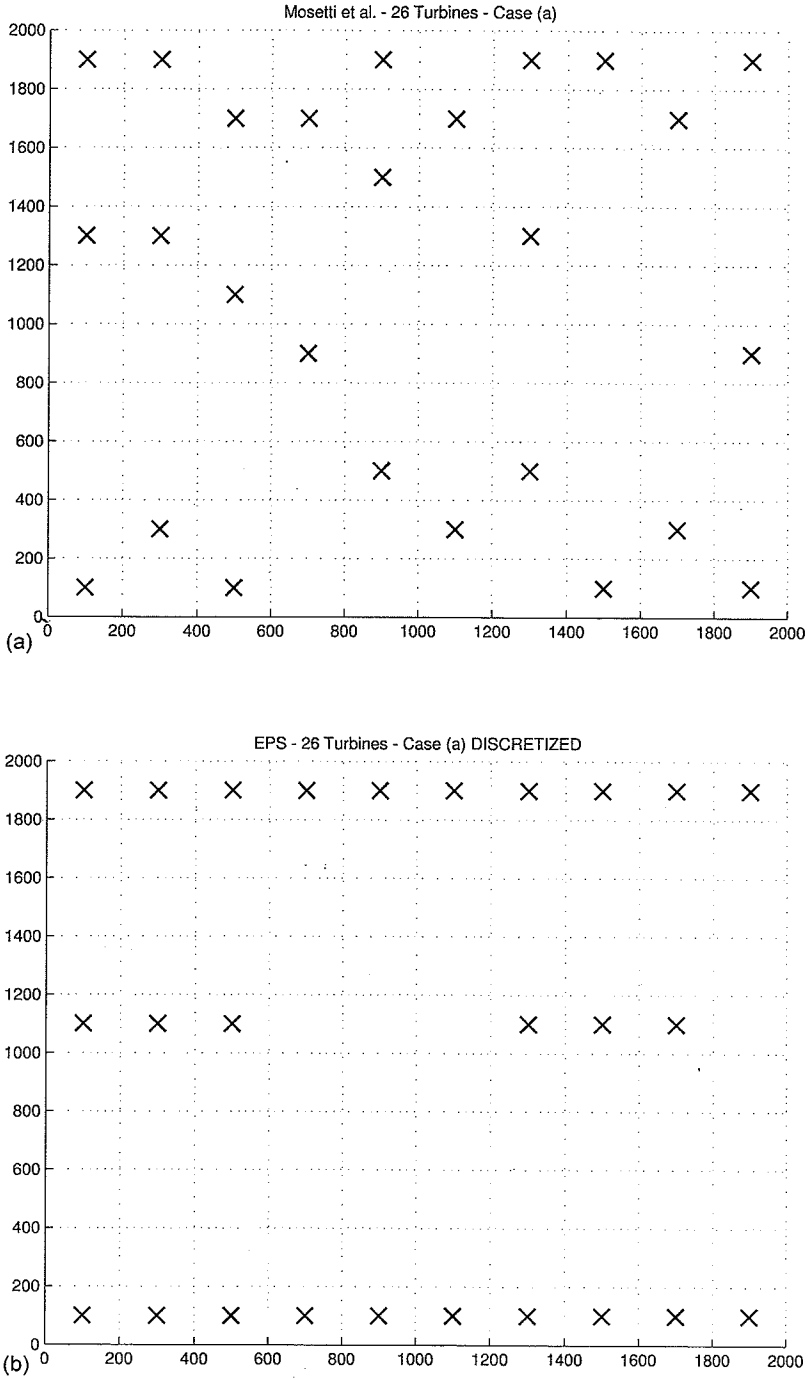

Fig. 6 (*a*) Mosetti et al.—26 turbine layout—case (a) and (*b*) discretized EPS - 26-turbine layout—case (a)

shown in Figs. 6(*a*) and 6(*b*), with quantitative comparison given in Table 1.

The results in Table 1 show that the EPS developed a better-performing layout within the discretized solution space than Mosetti et al.'s genetic algorithm approach. This implies that the capability of the EPS algorithm may actually be superior to that of this specific GA, aside from the fact that the EPS is otherwise designed to be utilized within a continuous solution space.

However, subsequent researchers who have solved this instance of the wind farm layout problem using this same discretized solution space have achieved a superior layout than Mosetti et al. while employing similar evolutionary algorithms. These researchers (Grady et al. [4], Bilbao and Alba [8], and Huang [9]) had identical case (a) results for each of their algorithms, a 30-turbine layout consisting of three straight lines of turbines, perpendicular to the onset direction of wind. The discretized EPS result duplicated this same layout. This 30-turbine layout has the best objective evaluation for a range of turbine numbers (in the case of the

Table 1 Comparison of Mosetti et al. and discretized EPS—case (a)

Result	Mosetti et al.	Discretized EPS
Objective function evaluation	0.0016197	0.00156225
Total power (kW)	12352	12806.2
N	26	26
Efficiency (%)	91.64	95.01

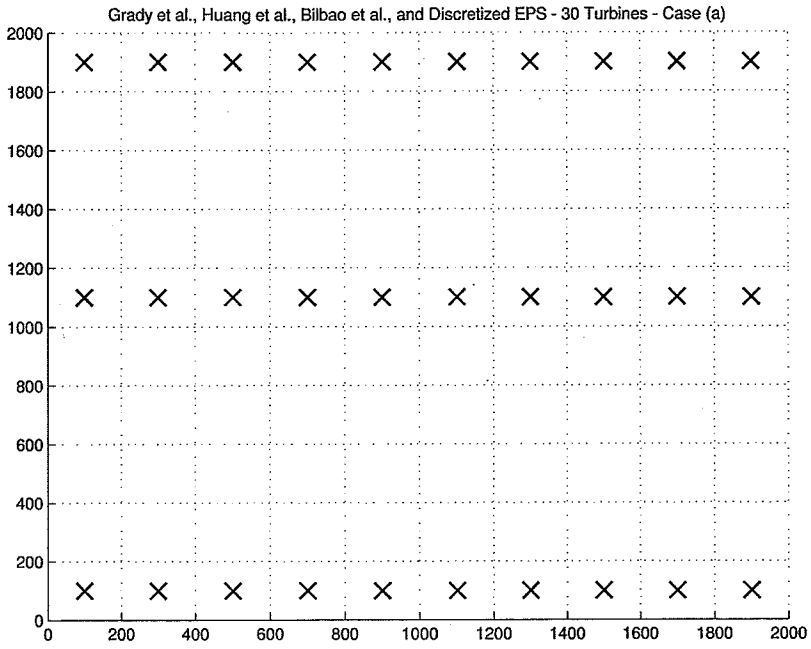

Fig. 7 Grady et al., Huang, Bilbao and Alba, and discretized EPS - 30 turbines—case (a)

Table 2 Comparison of Mosetti et al. and current EPS approach—case (a)

Result	Mosetti et al.	Mosetti et al. re-evaluation	Current EPS
Objective function evaluation	0.0016197	0.00158985	0.00148433
Total power (kW)	12,352	12583.8	13478.4
N	26	26	26
Efficiency (%)	91.64	93.36	100
Discrepancy (%)		1.87	

discretized EPS, from 15 turbines to 50 turbines), and is assumed to be the best layout possible for the coarseness of the discretization. This layout is given in Fig. 7.

This result shows that compared to evolutionary algorithms that exceed the initial result of Mosetti et al.'s genetic algorithm, the extended pattern search performs just as well, consistently converging on the best layout possible given the discretization. As the EPS is designed to use a continuous solution space, this will allow the already-comparable algorithm to outperform those which are limited by the necessity of a discretized grid. Subsequent reported layouts for the extended pattern search algorithm are no longer constrained by this discretized solution space.

Case (a). Comparisons to the Mosetti et al. Genetic Algorithm approach are compiled in Table 2. Visual representation of the 26-turbine Mosetti et al. layout was given in Fig. 6(*a*), and an example of a 26-turbine EPS-developed layout is included in Fig. 8.

Comparisons to the Grady et al. genetic algorithm approach [4] are compiled in Table 3, with the visual representation of the 30-turbine Grady et al. layout included previously in Fig. 7, and an example of a 30-turbine EPS developed layout included in Fig. 9.

The distributed genetic algorithm developed by Huang and the simulated annealing algorithm developed by Bilbao and Alba have identical case (a) layouts to the Grady et al. Genetic Algorithm approach shown in Fig. 7. However, their individual optimizations gave slightly different results than those reported by Grady et al., and as such are duplicated in Table 4. The re-evaluation from Table 3 remains consistent for both the simulated annealing and distributed genetic algorithm approaches.

As the specific means of calculation of the objective function in previous literature is not precisely given, out of fairness of comparison the layouts of previous studies were tested using the current wake model evaluation, and as such exhibit a slight discrepancy from the original reported result. For the Mosetti et al. and Grady et al. results, this discrepancy is 1.87% and 1.38%, respectively, indicating convincing consistency between evaluation models. However, the new evaluation of layouts from Marmidis et al. exposes dissimilarity in modeling (a 35.386% discrepancy). Studies of their results indicate a likely error in their reported data (for example, a theoretically impossible efficiency greater than 100% with turbines placed in the wakes of others). Therefore, comparison to this reference will not be included.

For case (a), the extended pattern search algorithm is able to create multiple 100% efficient layouts for trials that employ up to 43 turbines. Therefore, in comparison to both the 26-turbine Mosetti et al. result and the 30-turbine Grady et al. result, the current extended pattern search algorithm creates more efficient layouts that develop more power.

To determine the number of turbines that should be included in the reported EPS optimal layout for case (a), a plot of objective function evaluation versus the number of turbines is generated from EPS trials, shown in Fig. 10. The curve marked by circles represent the actual EPS trial data (with a polynomial fit superimposed), and the curve marked by squares indicates theoretical 100% efficient objective function evaluations.

The 4th-order polynomial fit of the objective function evaluation versus N(number of turbines) curve gives the following equation:

$$y = 7.798 \cdot 10^{-11}(x^4) - 2.037 \cdot 10^{-8}(x^3) + 2.012 \cdot 10^{-6}(x^2) - 8.826 \cdot 10^{-5}(x) + 0.003 \quad (10)$$

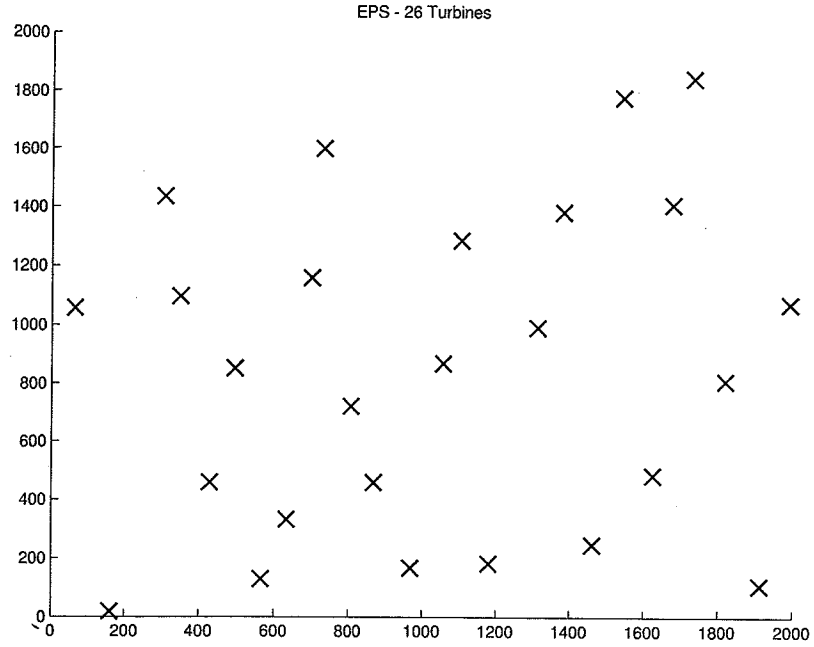

Fig. 8 EPS 26-turbine layout—case (a)

Table 3 Comparison of Grady et al. and current EPS approach—case (a)

Result	Grady et al.	Grady et al. re-evaluation	Current EPS
Objective function evaluation	0.0015436	0.00152255	0.00142032
Total power (kW)	14,310	14507.8	15552
N	30	30	30
Efficiency (%)	92.01	93.29	100
Discrepancy (%)		1.38	

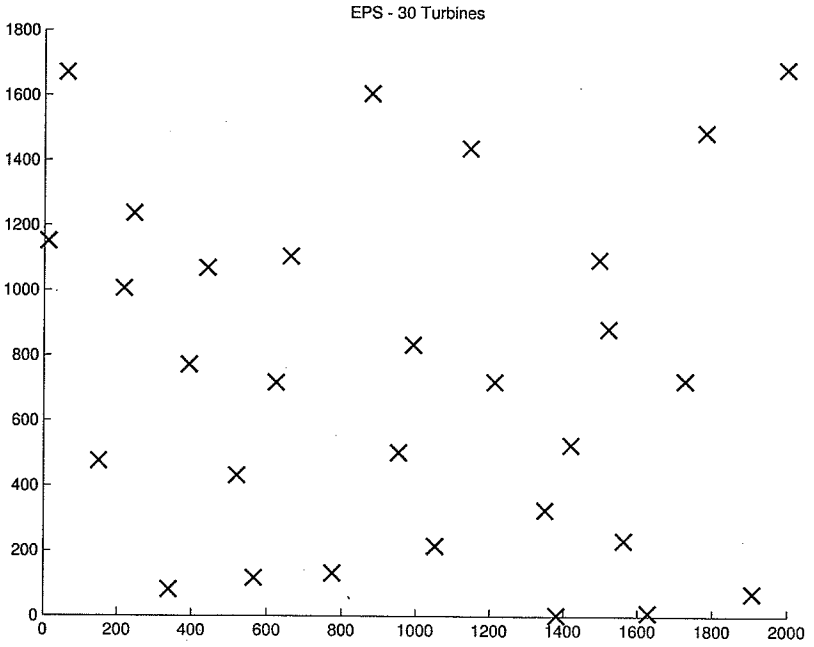

Fig. 9 EPS 30-turbine layout—case (a)

The minimum value of this curve is the estimation of the best objective function evaluation for any number of turbines. The value of x that minimizes this function is $x \simeq 54$. Therefore, the estimated optimal result of the extended pattern search is obtained by developing a 54-turbine layout, shown in Fig. 11. This layout develops 27,823 kW of power and is 99.39% efficient. The power and efficiency are derived from the objective function which, for the best case, had a value of 0.00129793. Among the ten runs the

Table 4 Comparison of Huang and Bilbao and Alba to current EPS—case (a)

Result	Huang	Bilbao and Alba	Current EPS
Objective function evaluation	N/A	N/A	0.00142032
Total power (kW)	14118	14205	15552
N	30	30	30
Efficiency (%)	90.78	91.36	100.00

mean objective value was 0.001301258 and the standard error of the mean was 4.55711×10^{-7}. Although this layout is less than 100% efficient, the design is still the most cost effective for the power generated based on the overall objective function evaluation.

For case (a), the EPS layouts created for larger numbers of turbines (including the 54-turbine layout in Fig. 11) reveal distinct patterns of placement; primarily long vertical "strings" of turbines

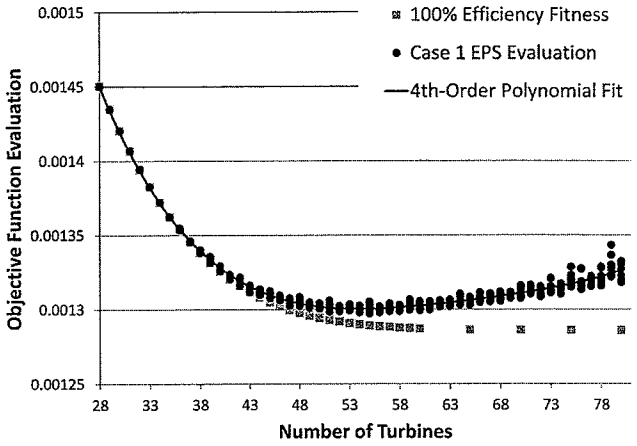

Fig. 10 Objective function evaluation versus number of turbines—case (a)

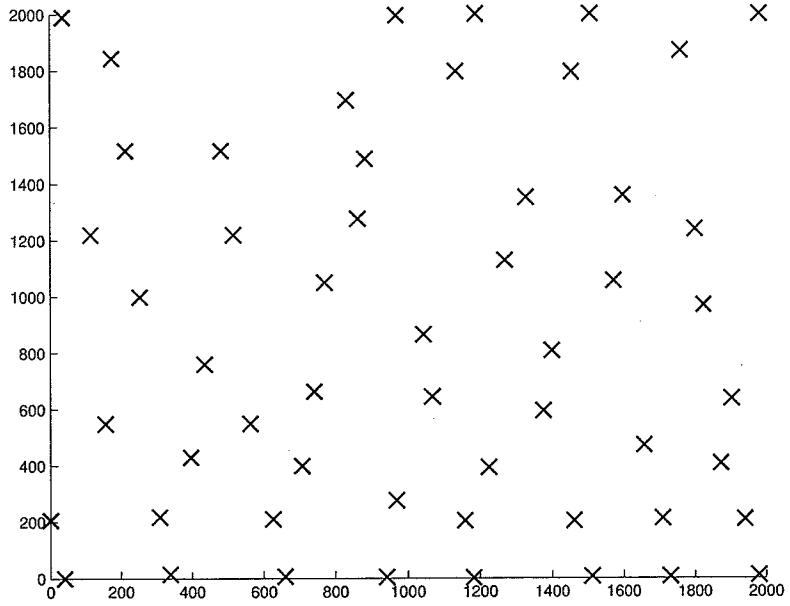

Fig. 11 Optimal 54-turbine EPS layout—case (a)

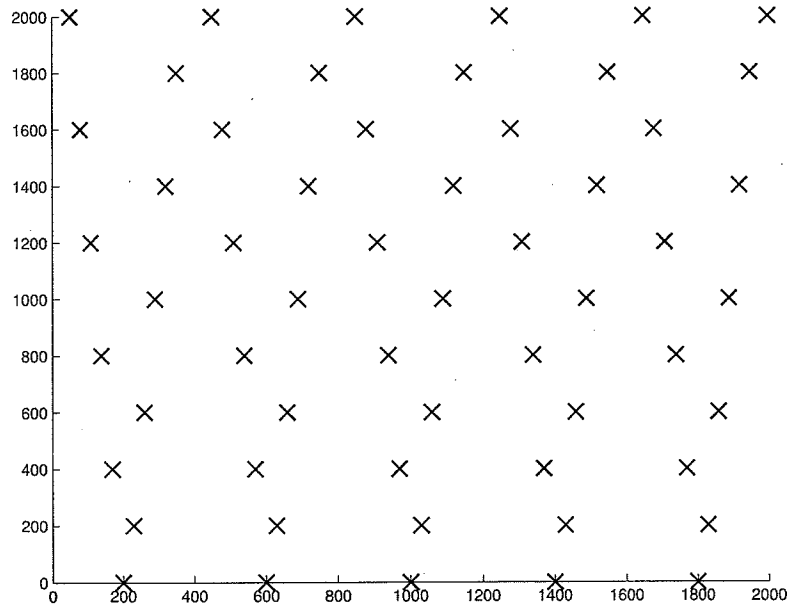

Fig. 12 100% efficient 56-turbine layout—case (a)

Table 5 Comparison of Mosetti et al. and current EPX approach—case (b)

Result	Mosetti et al.	Mosetti et al. re-evaluation	Current EPS
Objective function evaluation	0.0017371	0.00169916	0.00164384
Total power (kW)	9244.7	9443.5	9761.3
N	19	19	19
Efficiency (%)	93.86	95.88	99.10
Discrepancy (%)		2.10	

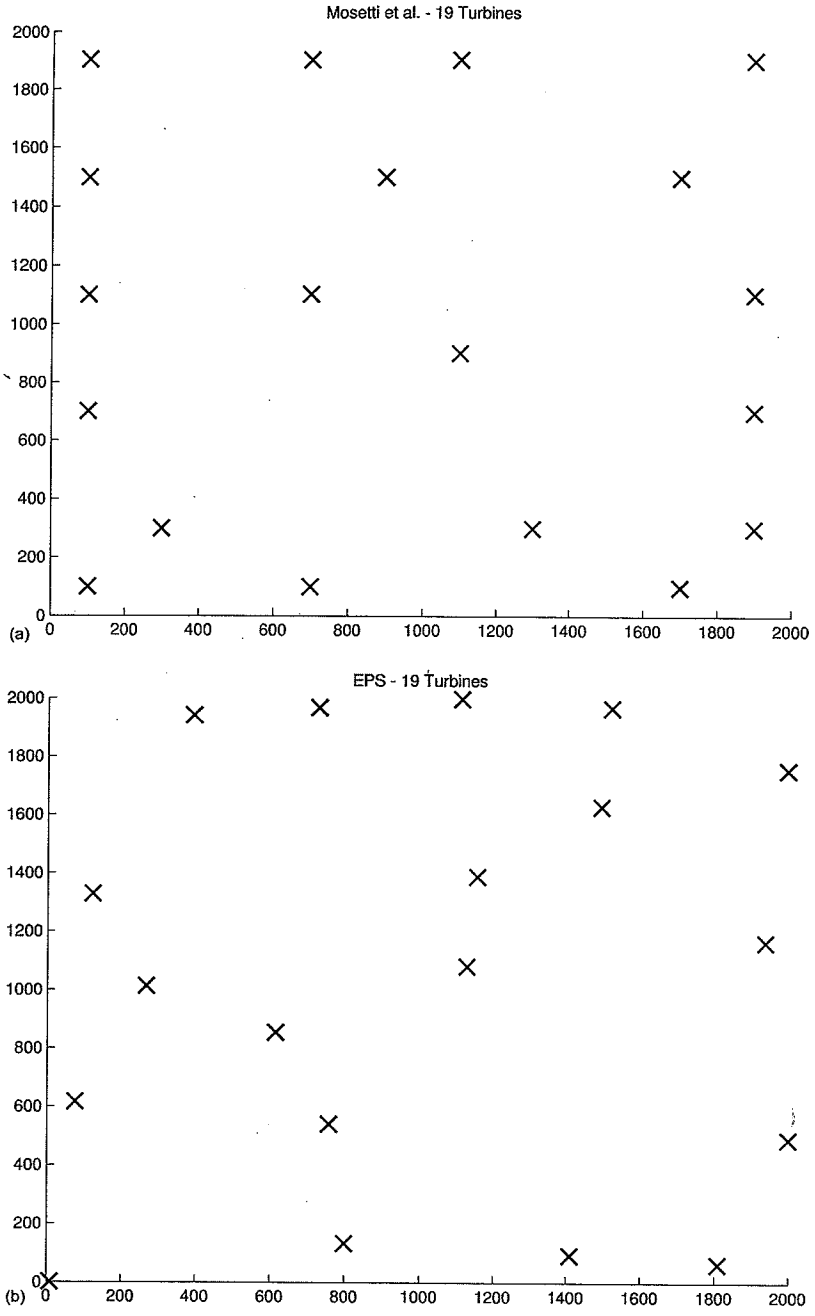

Fig. 13 (*a*) Mosetti et al. 19-turbine layout—case (b) and (*b*) and EPS 19-turbine layout—case (b)

Table 6 Comparison of Grady et al. and current EPS approach—case (b)

Result	Grady et al.	Grady et al. re-evaluation	Current EPS
Objective function evaluation	0.0015666	0.00146355	0.00139123
Total power (kW)	17220	18394.8	19351
N	39	39	39
Efficiency (%)	85.17	90.98	95.78
Discrepancy (%)		6.40	

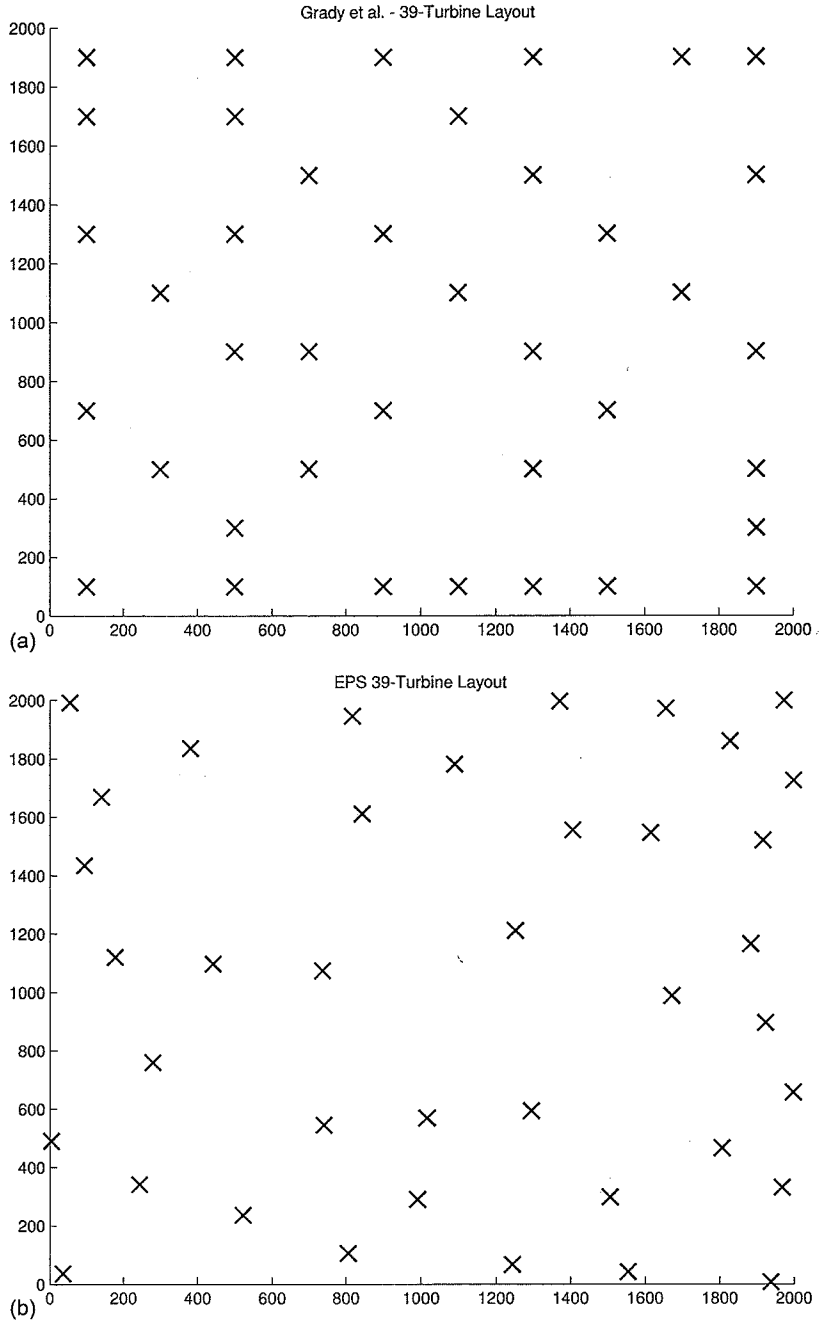

Fig. 14 (*a*) Grady et al. 39-turbine layout—case (b) and (*b*) EPS 39-turbine layout—case (b)

placed on slight diagonals, often forming "W" shapes. Based on the shapes identified in these solutions, a layout was manually developed as a heuristic derived from the EPS algorithm results, specifically for the case (a) wind conditions. A plot of the 100% efficiency objective function value versus the number of turbines (given in Fig. 10) shows an asymptotic approach to a minimum fitness value. It appears that the curve begins this asymptotic behavior near N=56, which indicates that the addition of more turbines above this number does not significantly benefit the objective function evaluation. Therefore the manually developed

Table 7 Comparison of Huang and current EPS—case (b)

Result	Huang	Huang re-evaluation	Current EPS
Objective function evaluation	N/A	0.00147015	0.00139826
Total power (kW)	15040.28	17553.1	18455.7
N	37	37	37
Efficiency (%)	78.41	91.51	96.22
Discrepancy (%)		14.30	

layout (Fig. 12) includes 56 turbines, exhibits 100% efficiency, and develops 29,030.4 kW of power.

Case (b). The second wind case is also that of constant wind speed (12 m/s), but now includes the more realistic approach of varying the wind onset angle. In 10-degree increments, 36 different rotational angles are considered, which allows for a thorough test of the solution space. The solution for the individual 36 angles are equally weighted and combined. Comparisons of the current EPS algorithm, along with re-evaluation of the Mosetti et al. layout using the current model, are found in Table 5. Visual representations of both the Mosetti et al. case (b) 19-turbine layout and an example of a 19-turbine EPS layout are shown in Figs. 13(*a*) and 13(*b*), respectively.

The EPS-developed 19-turbine layout for the multidirectional, constant wind speed case shows behavior of turbine migration toward the outer edges of the field. This behavior implies the algorithm is attempting to place turbines as far away from each other as possible to maximize their effective wind speed from all angles.

Similarly, Table 6 shows the Grady et al. result for case (b), the re-evaluation of the Grady et al. layout using the current model, and an example EPS result for the same number of turbines, for comparison purposes.

As indicated by Figs. 14(*a*) and 14(*b*), the behavior of the turbines for this higher-N layout differs from that of the previous 19-turbine layout. Instead of primary migration toward the outside of the field, the turbines are generally avoiding being placed in straight lines from all directions.

The simulated annealing algorithm developed by Bilbao and Alba uses the distributed genetic algorithm performed by Huang as a framework for comparison, and as such both case (b) and case (c) results for these works have the same number of turbines. As such, the comparison of these algorithms to the current EPS algorithm will be shown in combination, to avoid the duplication of figures. The comparison to Huang DGA work is shown in Table 7, and the comparison to Bilbao and Alba SA work in Table 8.

Visual representations of the case (b) layouts of Huang, Bilbao and Alba, and the current EPS for 37 turbines are shown in Figs. 15(*a*)–15(*c*), respectively.

The optimal EPS layout can be found using the same means as presented in the case (a). The case (b) trial data were plotted to show the change in objective function value as a function of the number of turbines. Figure 16 presents the 4th-Order polynomial fit of this data.

$$y = 1.497 \cdot 10^{-10}(x^4) + 1.840 \cdot 10^{-8}(x^3) - 3.741 \cdot 10^{-7}(x^2) - 2.277 \cdot 10^{-5}(x) + 0.0021 \quad (11)$$

The resulting curve has a minimum value at approximately 44 turbines.

An example of a 44-turbine EPS layout for case (b) is shown in Fig. 17. This 44-turbine case (b) EPS layout is 94.67% efficient and develops 21594.9 kW. The objective function evaluation for this case was 0.00138174, representing the best of ten trials with a mean objective value of 0.001387082 and standard error of the mean 9.91866×10^{-7}.

Case (c). The final case explored is multidirectional, varying wind speed. The three possible wind speeds are 8 m/s, 12 m/s, and

Table 8 Comparison of Bilbao and Alba and current EPS—case (b)

Result	Bilbao and Alba	Bilbao and Alba re-evaluation	Current EPS
Objective function evaluation	N/A	0.00147115	0.00139826
Total power (kW)	15268.84	17541.2	18455.7
N	37	37	37
Efficiency (%)	79.60	91.45	96.07
Discrepancy (%)		12.95	

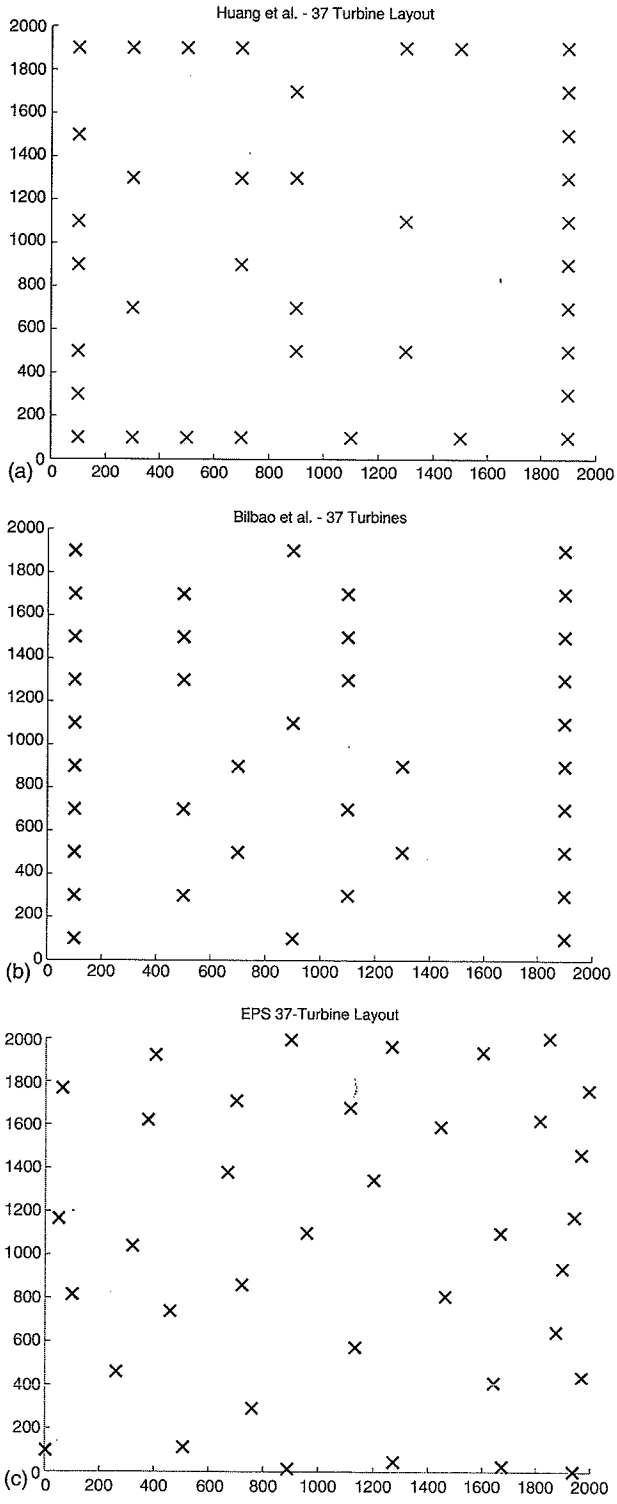

Fig. 15 (*a*) Huang 37-turbine layout—case (b), (*b*) Bilbao and Alba 37-turbine layout—case (b), and (*c*) EPS 37-turbine layout—case (b)

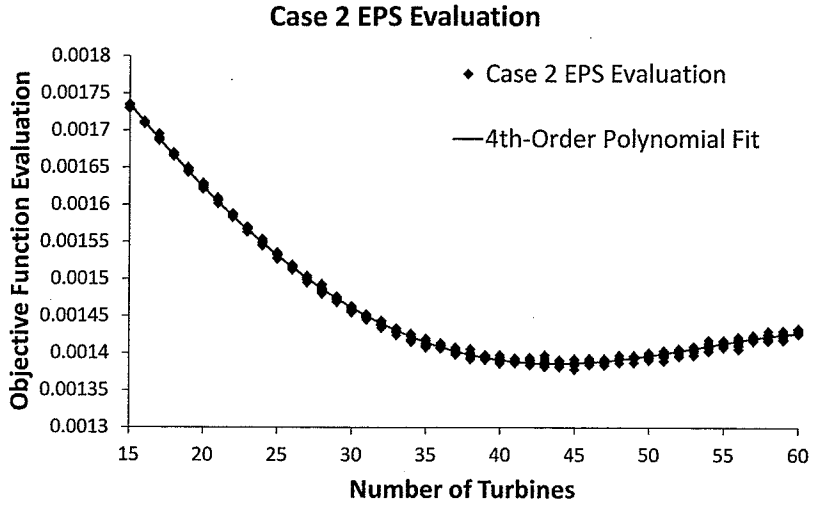

Fig. 16 Objective function evaluation versus number of turbines—case (b)

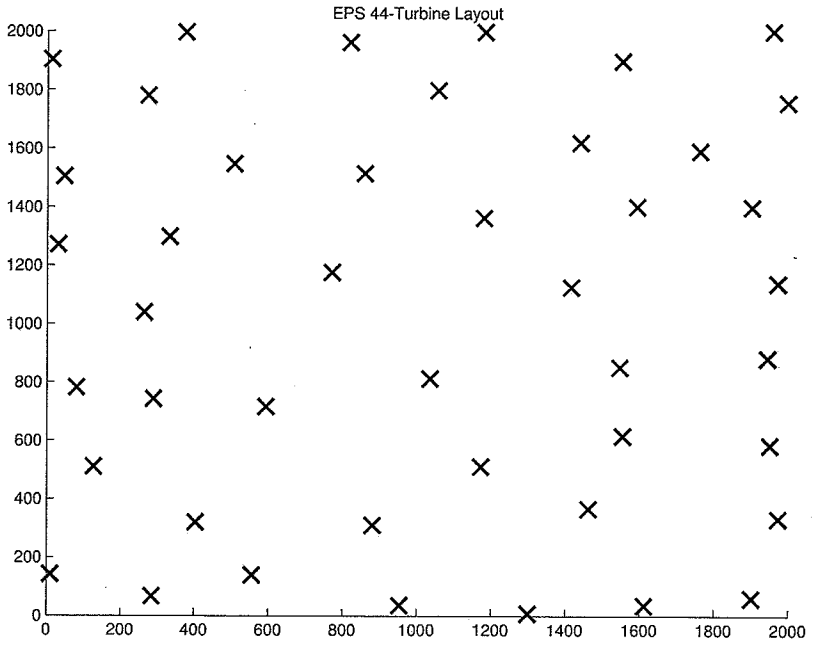

Fig. 17 Optimal 44-turbine EPS layout—case (b)

17 m/s. As with case (b), all 36 angular directions are considered (again occurring in 10-degree increments), however, in case (c) these directions and the wind speeds for each direction are weighted to model prominent wind directions. The fraction of occurrence (weighting) of each wind direction and wind speed are depicted in bar graph given in Fig. 18.

The multidirectional, varying wind speed case presents the opportunity to gauge the performance of these algorithms in a more realistic wind environment. Table 9 summarizes this performance for the 15-turbine Mosetti et al. result for case (c), as well as an example of a 15-turbine EPS result. Plots of both of these layouts are given in Figs. 19(*a*) and 19(*b*).

EPS-developed layouts for 15 and similarly small numbers of turbines exhibit no obvious patterns or movement behaviors. However, increasing the number of turbines, as with the following comparison of the results of the Grady et al. layout and EPS-developed layout for 39 turbines, does reveal visually clear placement patterns. The results of these two studies are summarized in Table 10, and Figs. 20(*a*) and 20(*b*) visually represent the two layouts.

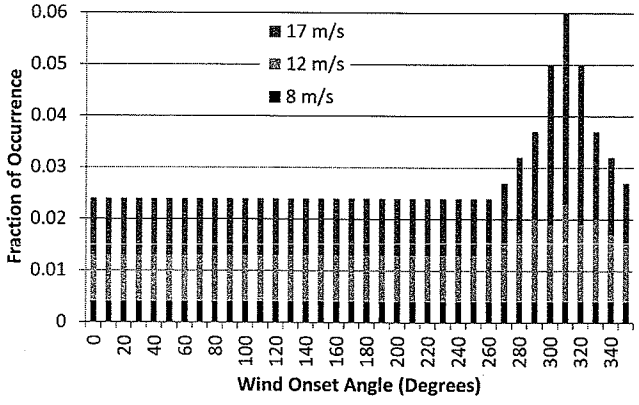

Fig. 18 Bar graph of weighting fractions—case (c)

Table 9 Comparison of Mosetti et al. and current EPS approach—case (c)

Result	Mosetti et al.	Mosetti et al. re-evaluation	Current EPS
Objective function evaluation	0.00099405	0.000984478	0.00096445
Total power (kW)	13460	13591.2	13873.4
N	15	15	15
Efficiency (%)	96.66	97.60	99.63
Discrepancy (%)		0.97	

Table 10 Comparison of Grady et al. and current EP approach—case (c)

Result	Grady et al.	Grady et al. re-evaluation	Curre EPS
Total power (kW)	32038	32491.9	34650
N	39	39	39
Efficiency (%)	88.49	89.74	95.7
Discrepancy (%)		1.39	

The comparison of the case (c) results of the EPS algorithm to those of Huang's DGA and Bilbao and Alba's SA show the behavior and movement of the turbines for an even greater number of turbines. Numerical comparison of the results is given for the DGA (Table 11) and SA (Tab 12) approaches.

There is a larger discrepancy between the DGA and SA r evaluations and the results stated in the literature. This may b caused by the incorporation of an idealized power mod

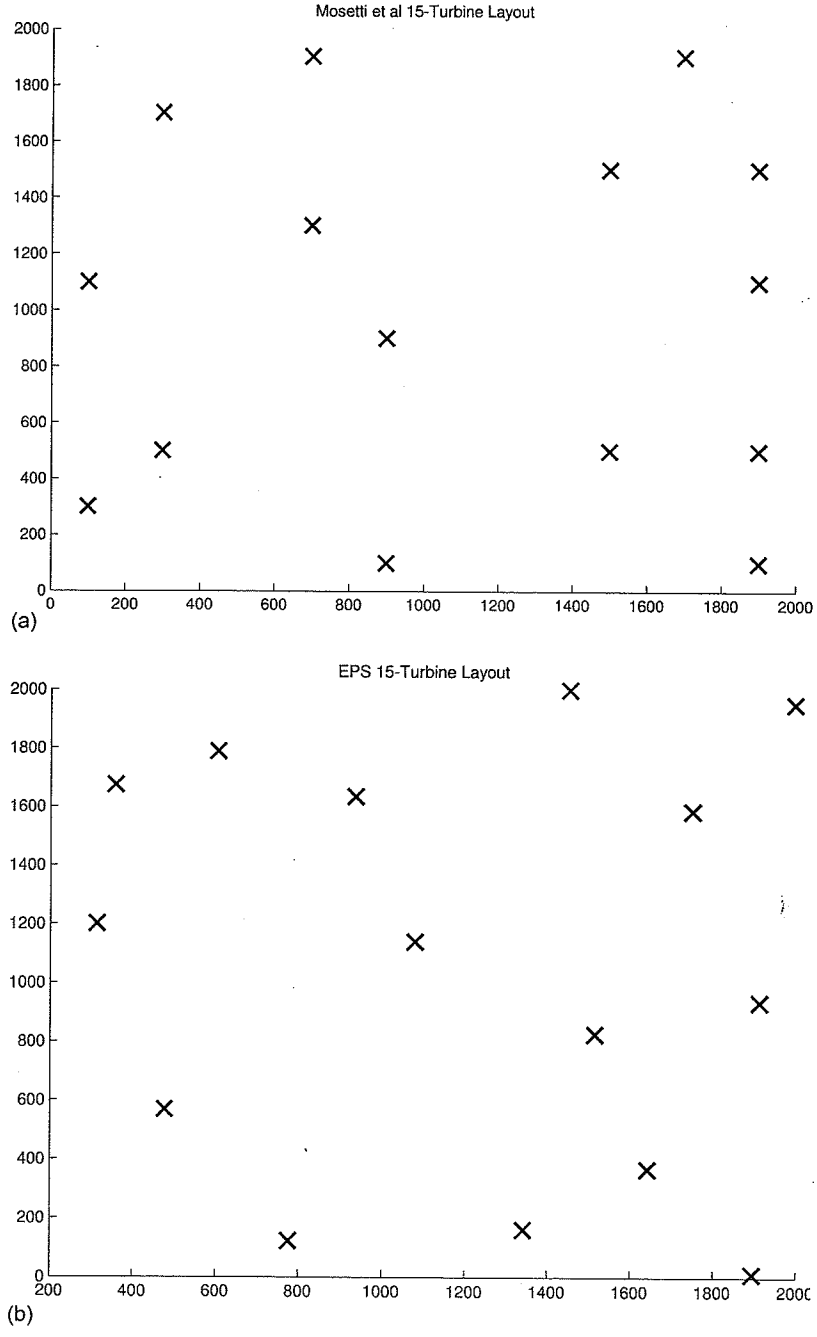

Fig. 19 (*a*) **Mosetti et al. 15-turbine layout—case (c) and** (*b*) **EPS 15-turbine layout—case (c)**

Table 11 Comparison of Huang and current EPS—case (c)

Result	Huang	Huang re-evaluation	Current EPS
Objective function evaluation	N/A	0.00138859	0.000774479
Total power (kW)	20430.7	22806.4	40890.5
N	47	47	47
Efficiency (%)	83.87%	52.27%	93.72%
Discrepancy (5)		10.41%	

(developed by Huang) that does not consider the power development of sacrificial turbines—turbines that evaluate to have negative effective wind speeds. The power developed by any turbine with a wind speed below 2 m/s and above 18 m/s is considered to be zero. Additionally, the power calculation given in Eq. (7) is only applied to those turbines whose effective wind speed is between and including 2 m/s and 12.8 m/s. The range constraints of the Huang power model are given below

$$P_i(\text{kW}) = \begin{cases} 0 & \text{for} \quad U_i < 2^{\text{m}}/_{\text{s}} \\ 0.3U_i^3 & \text{for} \quad 2^{\text{m}}/_{\text{s}} \le U_i \le 12.8^{\text{m}}/_{\text{s}} \\ 629.1 & \text{for} \quad 12.8^{\text{m}}/_{\text{s}} < U_i \le 18^{\text{m}}/_{\text{s}} \\ 0 & \text{for} \quad U_i > 18^{\text{m}}/_{\text{s}} \end{cases} \tag{12}$$

Lack of information regarding the use of this model versus the power development calculation given by Mosetti et al. could potentially be the cause of the larger discrepancy between the

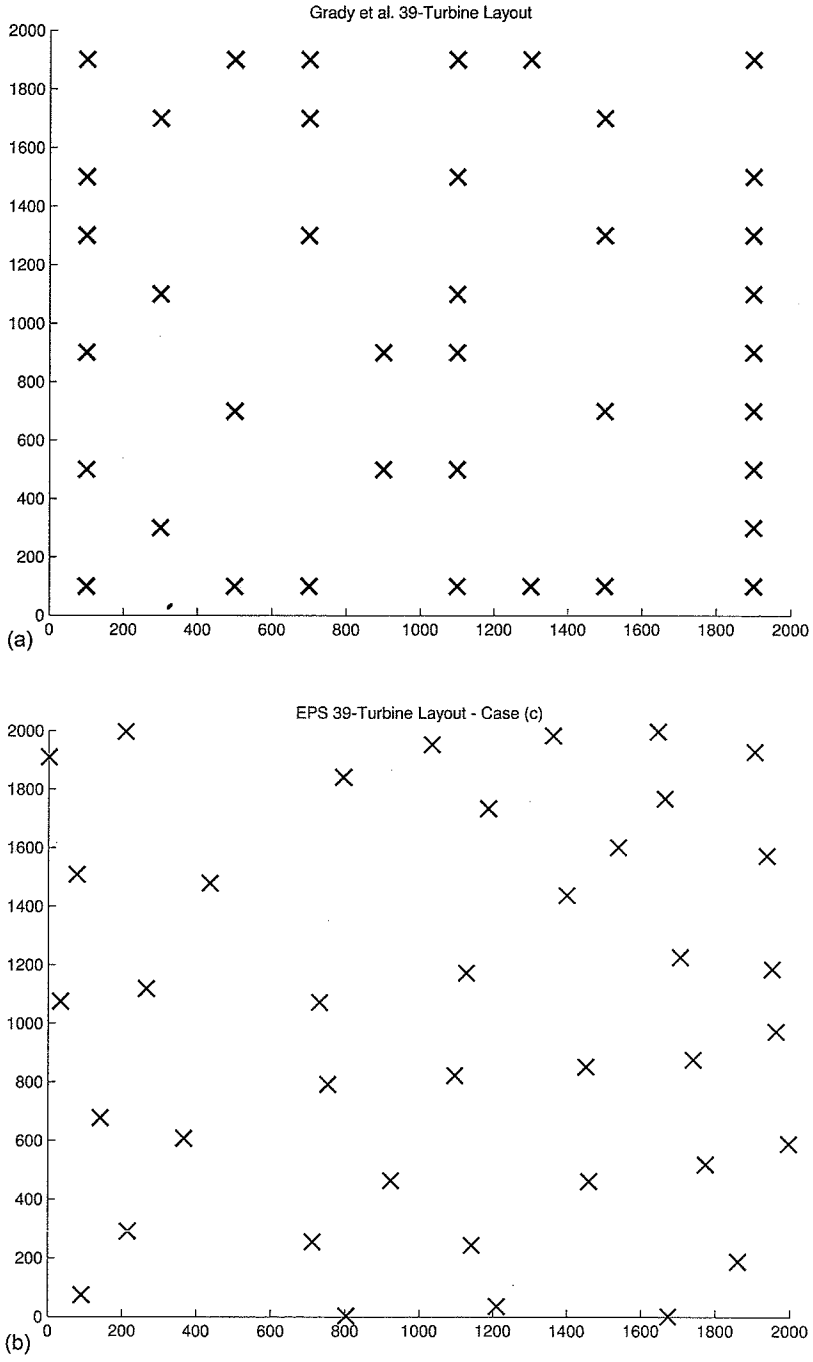

Fig. 20 (*a*) Grady et al. 39-turbine layout—case (c) and (*b*) EPS 39-turbine layout—case (c)

Table 12 Comparison of Bilbao and Alba and current EPS—case (c)

Result	Bilbao and Alba	Bilbao and Alba re-evaluation	Current EPS
Objective function evaluation	N/A	0.00138127	0.000774479
Total power (kW)	21025.84	22927.3	40890.5
N	47	47	47
Efficiency (%)	84.10	52.54	93.72
Discrepancy (%)		8.29	

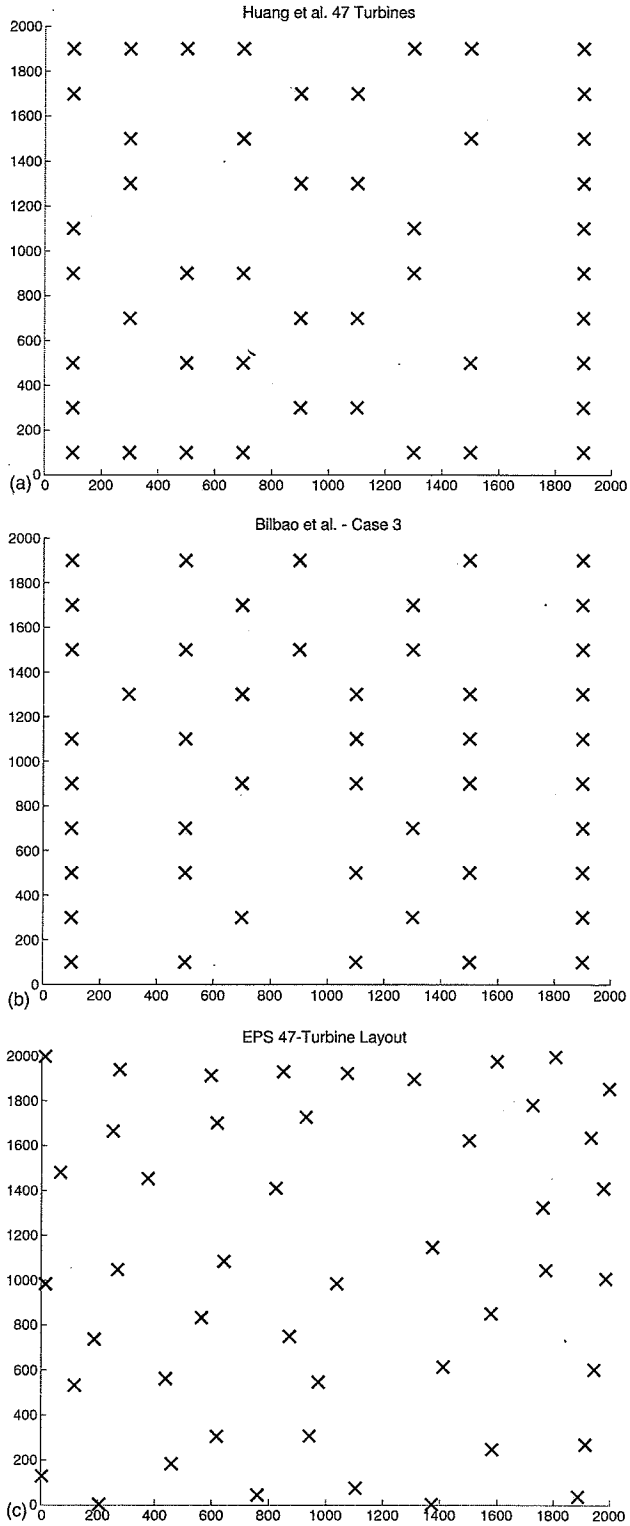

Fig. 21 (*a*) Huang 47-turbine layout—case (c), (*b*) Bilbao and Alba 47-turbine layout—case (c), and (*c*) EPS 47-turbine layout—case (c)

current re-evaluation and the stated previous results. The significant difference between the amount of power developed by the current EPS and both the powers developed by the DGA and SA algorithms suggests further divergence in model application. The plots for each the DGA, SA, and current EPS 47-turbine results for case (c) are shown in Figs. 21(*a*)–21(*c*), respectively.

The case (c) trial data was compiled and a plot of objective function evaluation as a function of the number of turbines was developed. As with the two previous cases, a 4th-order polynomial fit of the data creates a curve whose minimum suggests the optimal number of turbines for that case:

$$y = -7.834\,10^{-11}(x^4) + 9.493\,10^{-9}(x^3) - 1.692\,10^{-7}(x^2) - 1.350\,10^{-5}(x) + 0.0012 \quad (13)$$

The optimal number of turbines suggested for the case (c) EPS layout was 44. An example of a 44-turbine EPS layout for case (c) is shown in Fig. 22. This layout is 94.69% efficient and develops 38681.2 kW. The objective function for this best case had a value of 0.000771393; the mean objective value of ten trials was 0.000775204 and the standard error of the mean was 8.0704×10^{-7}.

Concluding Discussion

From these results, it is clear that the extended pattern search algorithm described is promising for these wind cases. It exhibits higher efficiency and develops more power than layouts presented in previous literature. The extended pattern search is also successful in that the conclusions drawn from resulting layouts influenced the manual development of high-N 100% efficient layout in case (a). For cases (b) and (c), the EPS was able to generate slightly higher efficiency and higher power-developing layouts; however, the behavior indicated by the turbine movement in these layouts suggests further exploration in the development of heuristic patterns that may lead to superior layouts for more complex wind cases. The first step in enabling this extended pattern search to be a viable choice for wind farm layout optimization is the incorporation realistic wind data. Additional attributes should also be considered, such as utilizing varying wake models and incorporating existing turbine geometry. Due to the fact that the layout problem is multimodal and a stochastic algorithm is employed, the EPS generated better performing layouts than the literature, though potentially not the global optima. This should be seen as an advantage; however, as the ability to select from multiple equally good layouts might better accommodate the dynamic conditions of a potential wind farm location. The generation of multiple optimal layouts also aids in the understanding of the models used and the behavior of the turbine movement, which enables the future development of heuristics and other extension to this work. Finally, the work demonstrates that algorithms used for product layout find application in wind farm layout design, enabling those advances to similarly advance the state of wind farm design. As the extended pattern search has proven to be an effective layout optimization algorithm for the wind farm design problem as compared to other approaches, in the future more sophisticated wake, power, and cost modeling can be incorporated into the EPS framework in an effort to design more real-world applicable wind

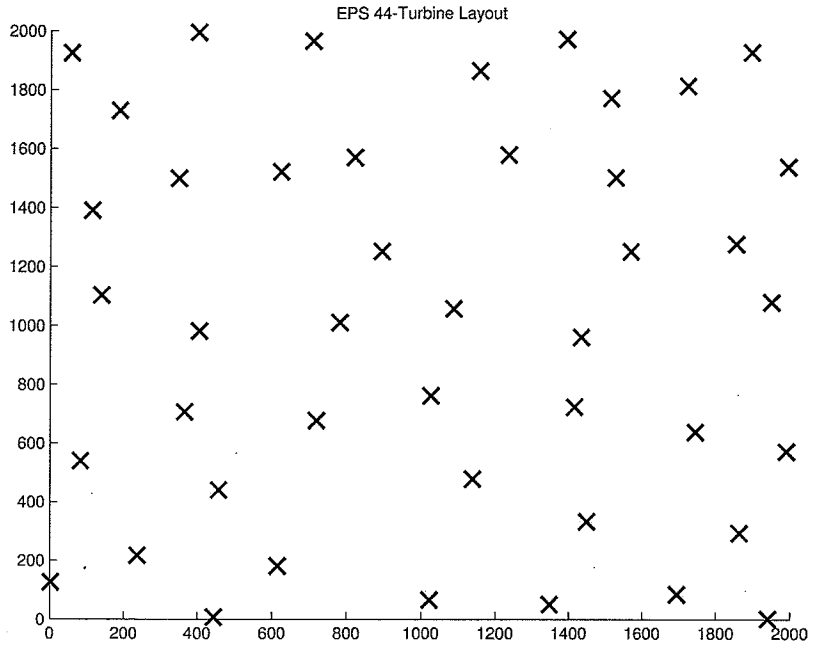

Fig. 22 Optimal EPS 44-turbine layout—case (c)

farms. As well, the efficiency of the algorithm can be tuned based on these more sophisticated models.

Acknowledgment

This work was funded by the National Science Foundation under Grant Nos. CMMI-0940730 and CMMI-0855326. The authors would like to thank Dr. Lindsay Landry for her guidance in this work.

References

[1] US Department of Energy, 2008, "Wind Energy by 2030: Increasing Wind Energy's Contribution to U.S. Electricity Supply," http://www.nrel.gov/docs/fy08osti/41869.pdf

[2] Mosetti, G., Poloni, C., and Diviacco, B., 1994, "Optimization of Wind Turbine Positioning on Large Wind Farms by Means of a Genetic Algorithm," J. Wind. Eng. Ind. Aerodyn., **51**(1), pp. 105–116.

[3] Jensen, N. O., 1983, *A Note on Wind Generator Interaction*, Risø National Laboratory, Roskilde, Denmark.

[4] Grady, S. A., Hussaini, M. Y., and Abdullah, M. M., 2005, "Placement of Wind Turbines Using Genetic Algorithms," Renewable Energy, **30**, pp. 259–270.

[5] Wan, C., Wang, J., Yang, G., and Zhang, X., 2009, "Optimal Siting of Wind Turbines Using Real-Coded Genetic Algorithms," European Wind Energy Conference and Exhibition (EWEC), Marseille, France.

[6] Mittal, A., 2010, "Optimization of the Layout of Large Wind Farms Using a Genetic Algorithm," Master's Thesis, Case Western Reserve University, Department of Mechanical Engineering, Cleveland, OH.

[7] Marmidis, G., Lazarou, S., and Pyrgioti, E., 2008, "Optimal Placement of Wind Turbines in a Wind Park Using Monte Carlo Simulation," Renewable Energy, **33**, pp. 1455–1460.

[8] Bilbao, M., and Alba, E., 2009, "Simulated Annealing for Optimization of Wind Farm Annual Profit," 2nd International Symposium on Logistics and Industrial Informatics (LINDI), Linz, Austria.

[9] Huang, H. S., 2007, "Distributed Genetic Algorithm for Optimization of Wind Farm Annual Profits," The 14th International Conference on Intelligent Systems Applications to Power Systems (ISAP), Kaohsiung, Taiwan.

[10] Elkinton, C. N., Manwell, J. F., and McGowan, J. G., 2006, "Offshore Wind Farm Layout Optimization (OWFLO) Project: Preliminary Results," *Proceedings of 44th AIAA Aerospace Science Meeting and Exhibit*, AIAA, Reno, NV.

[11] Sisbot, S., Turgut, O., and Tunc, M., 2009, "Optimal Positioning of Wind Turbines on Gokceada Using Multi-Objective Genetic Algorithm," Wind Energy, **11**(4), pp. 297–306.

[12] Emami, A., and Noghreh, P., 2010, "New Approach on Optimization in Placement of Wind Turbines Within Wind Farm by Genetic Algorithms," Renewable Energy, **35**(7), pp. 1559–1564.

[13] Kusiak, A., and Zheng, H., 2010, "Optimization of Wind Turbine Energy and Power Factor With an Evolutionary Computation Algorithm," Energy, **35**, pp. 1324–1332.

[14] Gonzalez, J. S., Rodriguez, A. G. G., Mora, C., Santos, J. S., and Payan, M. B., 2010, "Optimization of Wind Farm Turbines Layout Using an Evolutive Algorithm," Renewable Energy, **35**, pp. 1671–1681.

[15] Saavedra-Moreno, B., Salcedo-Sanz, S., Paniagua-Tineo, A., Prieto, L., and Portilla-Figueras, A., 2011, "Seeding Evolutionary Algorithms With Heuristics for Optimal Wind Turbines Positioning in Wind Farms," Renewable Energy, **36**(11), pp. 2838–2844.

[16] Chowdhury, S., Zhang, J., Messac, A., and Castillo, L., 2012, "Unrestricted Wind Farm Layout Optimization (UWFLO): Investigating Key Factors Influencing the Maximum Power Generation," Renewable Energy, **38**(1), pp. 16–30.

[17] Mustakerov, I., and Borissova, D., 2010, "Wind Turbines Type and Number Choice Using Combinatorial Optimization," Renewable Energy, **35**(9), pp. 1887–1894.

[18] Ituarte-Villarreal, C. M., and Espiritu, J. F., 2011, "Optimization of Wind Turbine Placement Using a Viral Based Optimization Algorithm," Procedia Comput. Sci., **6**, pp. 469–474.

[19] Yin, S., and Cagan, J., 2000, "An Extended Pattern Search Algorithm for Three-Dimensional Component Layout," J. Mech. Des., **122**(1), pp. 102–109.

[20] Aladahalli, C., Cagan, J., and Shimada, K., 2007, "Objective Function Effect Based Pattern Search—An Implementation for 3D Component Layout," J. Mech. Des., **129**(3), pp. 255–265.

[21] Manwell, J. F., McGowan, J. G., and Rogers, A. L., 2009, *Wind Energy Explained: Theory, Design, and Application*, 2nd ed., John Wiley and Sons, Chichester, UK.

[22] Katic, I., Hojstrup, J., and Jensen, N. O., 1986, "A Simple Model for Cluster Efficiency," European Wind Energy Association Conference and Exhibition. Rome, Italy.

[23] Torczon, V., and Trosset, M. W., 1998, "From Evolutionary Operation to Parallel Direct Search: Pattern Search Algorithms for Numerical Optimization," Comput. Sci. Stat., pp. 396–401.